Optimizing a parametric energy model for use in citywide residential overheating analysis

Seth H. Holmes[1], Nicholas B. Rajkovich[2], and Fahed Baker[3]

[1,3]University of Hartford, Department of Architecture, West Hartford, CT, USA

[2]University of Buffalo, Department of Architecture, Buffalo, NY, USA

Corresponding author email: sholmes@hartford.edu

Abstract

City-wide urban building energy modeling may help estimate which residential buildings in a city are at risk of occupant overheating during a heat wave. Six parametric energy modeling methods are presented for use in an automated analysis to generate energy models using existing building information or GIS data. An evaluation of the six methods generates models that mimic detailed energy models for three existing homes in Cleveland, Ohio, USA. A comparison of parametric to detailed models using R^2 and CV-RMSE indicates that five out of six models adequately represent the detailed models when analyzing operative temperature and wet-bulb globe temperature.

Introduction

As the climate changes, the risk of heat waves continues to increase for numerous cities around the world (Intergovernmental Panel on Climate Change, 2014). Furthermore, an unequally distributed risk of exposure to high indoor temperatures exists within many cities; heat wave events disproportionately affect elderly, minority, and low-income residents (ONeill & Ebi, 2009). In addition to these individual risk factors, contextual and microclimatic risk factors contribute to heat related morbidity and mortality; contextual factors include living in homes without air-conditioning, building age and construction type, building exposure to direct sun, access to natural ventilation, and living in neighborhoods with higher urban heat island effects (Reid, et al., 2009).

While several planning and health related studies created heat-related vulnerability maps at city-wide census tract level (Chuang & Gober, 2015; Reid, et al., 2009; Loughnan, Tapper, Phan, Lynch, & McInnes, 2013; Seroka, Kaiser, & Heany, 2011; Rosenthal, Kinney, & Metzger, 2014), to date no studies have examined the potential for residential overheating at the individual household level, also known as a parcel-level analysis. A parcel-level overheating study analyzes an individual building for indoor environmental conditions in relation to occupant overheating thresholds and metrics.

Architects and engineers use whole-building energy models to predict indoor environmental conditions as well as building energy consumption; these models also predict indoor occupant comfort and overheating in relation to existing comfort standards such as ASHRAE 55 and BS EN 7730 (ASHRAE, 2013; BSI, 2007). Whole-building energy models predict heat flow in and out of a building by combining numerous variables including historical weather data, building construction specifications, and occupant loads and schedules (US Department of Energy Building Technology Office, 2016). Indoor environmental outputs from an energy model include dry-bulb temperature, relative humidity, mean-radiant temperature, operative temperature, and in some cases air speed. Furthermore, using indoor environmental outputs from an energy model, a recent study by Holmes (2012) developed a method to calculate indoor wet-bulb globe temperature (WBGT), a standardized occupant heat-stress metric, to evaluate potential heat stress thresholds in an unconditioned building during summertime conditions (International Organization for Standardization, 1989). Urban planners evaluate unconditioned buildings and homes for occupant heat-stress vulnerability due to lower air-conditioning usage in vulnerable communities, older housing stock, and potential for heat wave induced electrical outages that render mechanical cooling useless (Building Resiliency Task Force, 2013). However, no study to date has attempted to predict indoor residential heat stress vulnerability across a city using a bottom-up energy modeling approach.

An analysis combining whole-building energy models with citywide property datasets from geographic information system (GIS) databases could provide urban planners and health officials with a more precise prediction and identification of vulnerable residences, which would help target building level design interventions. However, this type of citywide analysis requires tens, or even hundreds, of thousands of individual energy models to estimate interior heat stress vulnerability in residential buildings. Creating unique energy models and their surrounding features for each

residential building in a city requires excessive time and resources to implement, thus rendering such a task impractical. However, an analysis utilizing stock parametric models for a limited number of residential buildings reduces time and costs by eliminating redundant modeling and by linking the models to existing building information datasets; various studies illustrate the benefits of parametric modeling for energy model generation (Parker, et al., 2014; Ellis, 2016). Additionally, citywide parametric modeling methods are inherent to the growing field of urban building energy modeling or UBEM (Reinhart & Cerezo, 2016).

A citywide UBEM analysis could extract parametric model and contextual inputs from GIS datasets, generic building archetypal information databases similar to Europe's TABULA project (Inteligent Energy Europe, 2012), or from specific parcel-level building survey data. Model parameters can include building microclimatic data including parcel orientation, neighboring structures, vegetation, ground surface materials, building footprint geometry, floor area, number of floors, number or rooms, room type, building construction type, etc. The overall UBEM analysis inputs parcel data and "flexes" geometry and building archetype parameters accordingly to generate simulations for each residential building parcel; a recent study automatically generated models for residential buildings in Kuwait City using a similar process (Cerezo, Sokol, Reinhart, & Al-Mumin, 2015). With that said, 3D building geometry is not always present in GIS datasets; therefore building volumes are often extruded from 2D building footprints, as was done in a UBEM study for Westminster, England (Tian, Rysanek, Choudhary, & Heo, 2015). However, building geometries are not always simple extrusions with single-zone floors; often times more specific building information, such as floor areas and room quantities, is available from city building information databases. Utilizing higher resolution building construction and geometry data is crucial to occupant heat-stress vulnerability given that building shading, shape, construction, zone division, operation and loads directly affect a room's heat gain.

This paper compares a series of stock parametric energy models for potential use in an UBEM overheating vulnerability analysis that would utilize 2D GIS geometry information, building survey information, and archetypal data for single-family homes as inputs for the parametric models. The model comparison includes a case study of three single-family homes in Cleveland, Ohio, USA that incorporates model inputs from a local building survey information database (Cuyahoga County, 2016).

Methodology

The method developed for evaluating the stock parametric models for use in an UBEM overheating analysis includes the following steps; the remainder of this section further defines each step:

1) Specify building datasets and model parameters,
2) Define/create multi-zone parametric energy models,
3) Select and model baseline building(s),
4) 'Flex' stock parametric models to represent baseline,
5) Calculate heat stress values from simulation outputs,
6) Compare accuracy of stock models with baseline.

1) Specify building datasets and model parameters

A typical US city has a unique set of existing building data available through GIS, archetypal databases and existing building surveys; for this study, the authors identified the following mix of building variables for use with some or all of the tested stock parametric models:

- GIS data include 2D building dimensions, and footprint shape, and building orientation.
- Exact building survey information include building height, floor quantities, floor areas, room types, room quantities, roof design type, attic (Y/N), and wall/roof assembly types (age and quality).
- Building archetypal assumptions include glazing assemblies (types, size, and quantity), wall/roof construction for each assembly type, residential occupancy and schedules, plug, and lighting loads.
- Cooling system assumptions include no air conditioning and windows operation (open/closed).
- Shading from adjacent buildings and trees are not included in this study in an effort to evaluate all parametric design types for 'worst case scenario' overheating.

Each stock parametric energy model has specific values defined for each building design parameter.

2) Define and create stock parametric energy models

The authors developed a series of parametric modeling categories and sub-types for the overheating UBEM analysis to reflect various combinations of building information inputs that might be available for any given US city. For example, a city might have GIS data for building footprints as well as existing building survey data for floor quantities and areas; with this information, a parametric model can extrude a first floor volume and then use the survey data to adjust the envelope perimeter for the 2nd floor shape and area.

Three modeling categories represent combinations of GIS and building survey datasets potentially available to a typical UBEM study: Category 1 includes GIS dimensions but no building survey data; Category 2 includes survey data but no GIS Dimensions or similar CAD footprint data; and Category 3 includes GIS dimensions and building survey data. Each modeling category has two separate model types. Table 1 identifies the parameter combinations, assumptions, and calculations that distinguish each parametric modeling type; Table 2 also indicates the common variables used by all six of the model types. Each model is multi-zonal in order to estimate the hottest and coolest rooms in any given building analysis. The paragraphs below further explain the selection process for the model parameters and Figure 2 illustrates geometric relationships.

Table 1: Parameter combinations and data sources for all six models

	GIS bldg Footprint	1st floor shape	1st floor Area	Upper floor shape	Upper floor Area(s)	Zones/fl	Glazing qty	Upper floor Area(s)
1A	no	square	exact	same as 1st	same as 1st	4	Glazing 1	n
1B	no	square	exact	square	exact	4	Glazing 1	y
2A	yes	exact	exact	same as 1st	same as 1st	4	Glazing 2	n
2B	yes	exact	exact	same as 1st	same as 1st	4+	Glazing 2	n
3A	yes	exact	exact	exact	exact	4+	Glazing 2	y
3B	yes	simplified	simplified	simplified	simplified	4 to 9	Glazing 1	y

Key: Data source
- GIS dimensions
- Existing building survey
- Assumption (Static)
- Assumption (Calculated)

Table 2: Common variables used for all six models

U-Values (W/m^2K)							Internal Loads (W/m^2)		
Roof (insulated)	Roof (uninsul.)	Attic Floor	Ext. Wall	Basement Wall	Slab on Grade	Glazing	Occ.	Light	Equip.
0.169	2.938	0.165	0.304	3.329	3.295	7.01	0.06	0.191	0.228

Consistant assumptions, all models
1) Floor to Floor height = 2.67m (8.75 ft);
2) Glazed opening = 1.0 m^2(10.7 ft^2)
3) Shading = No; Natural Ventilation = N

For Category 1, model types 1A and 1B do not utilize specific GIS or CAD footprint data, so the two model types utilize square footprint shapes based on floor area data from an existing building survey. The primary difference between 1A and 1B is the upper floor shapes; 1A simply uses an extruded shape from the 1st floor, whereas 1B uses floor area data for upper floors to determine the perimeter wall locations. The upper floor building volumes are also square shaped and centered above the 1st floor. For both model types, a 2x2 grid divides each floor plan into four equal, rectilinear zones; both models also use Glazing Method 1 to add one centered window per exterior wall per zone (i.e., eight windows per floor).

For Category 2, model types 2A and 2B utilize specific building footprint data from 2D GIS datasets to determine the model geometry for the first floor; potential upper floor geometry is a simple extrusion due to the lack of building survey information or 3D GIS data for this model category. The primary difference between 2A and 2B is the zone creation. Model 2A divides each floor plan into four zones based on two lines that intersect at the centroid of the floor. Model 2B has a baseline zone division equal to 2A; however it also generates internal zone boundaries 1) perpendicular to the perimeter wall wherever the wall jogs are ≥1m (3 ft.) and 2) if a zone wall is ≥ 6.5m (20 ft.) on any side. Glazing units are equally determined for both models using Glazing Method 2: 1) count exterior walls if plan length ≥ 2.6m (8 ft.), 2) add one window per exterior wall.

For Category 3, model types 3A and 3B also utilize building footprint data from 2D GIS datasets to determine the model geometry for the first floor; however the models utilize building survey data to calculate upper floor areas and zones. Model 3A uses building survey CAD data to determine upper floor footprints in relation to the lower floor footprint; the zoning and glazing process is the same as described for Model 2B. Model 3B is unique in that it simplifies GIS footprint plan for houses with mostly rectilinear plans. The 3B model is comprised of four zones in a 2x2 arrangement. The model's algorithm reads length and width dimensions from a GIS plan to determine if the building is rectangular (ignoring wall bulges/alcoves ≤ 1m (3 ft.) and, if so, generates a 4-zone model using model type 1B's method. If a non-rectangular (i.e., L-shaped) building is determined, additional zones are added outward of, but in line with, the 2x2 grid. The maximum building arrangement possible for the 3B model is a 3x3 grid of zones minus one zone (a complete rectangle would simply be a 2x2 zone grid model). Model 3B uses Glazing Method 1 to determine windows.

Table 2 illustrates the common variables present in all six models. Though the models are capable of receiving construction inputs, this paper presently normalizes the models for construction assemblies and roof types; the construction types utilized represent a 1980-Era U.S. home. Similarly, the roof type is a simple extruded 1.5m (4.5 ft.) tall attic volume with a flat roof.

The energy modeling engine used in this paper is EnergyPlus in conjunction with the Archsim energy modeling parametric plug-in for Rhinoceros and Grasshopper (Robert McNeel & Associates, 2016; Dogan, 2016; US Department of Energy Building Technology Office, 2016).

3) Select and model case study baseline buildings

This study includes three baseline models representing three single-family homes in Cleveland, Ohio, USA as indicated in Figure 1 and Table 3. The city of Cleveland has approximately 400,000 residents and a metropolitan region with roughly 2,000,000 people; the city is located on the south shore of Lake Erie which keeps the region's Continental climate mild, but still exhibiting four distinct seasons. The baseline houses represent three distinct single-family home types: 1-story, split-level, and 2-story. For this study, a split-level house has significant single story and 2-story portions; the baseline and parametric models assume floor plates align between the 1-story and 2-story portions. To optimize the baseline home geometry, the authors monitored indoor and outdoor dry-bulb temperature (TA) and relative humidity (RH) for each home during the summer of 2013. Validation simulations for each baseline model utilize a customized energy plus weather file (EPW) that include onsite recorded weather data (TA and RH) combined with historical weather data recorded at the nearby Hopkins international airport (White Box Technologies, 2016). Validation simulations compare recorded indoor

Figure 1: Baseline single-family houses

temperature data with modeled data using linear correlation (R^2) and the coefficient of variation of the root mean squared error (CV-RMSE) based on ASHRAE standard 14 (ASHRAE, 2014).

For the comparison between parametric and baseline models, each baseline energy model retains its existing layout information, window locations, and roof form. However, regarding wall and roof construction, the comparison normalizes construction variables and therefore modifies each baseline energy model to include the same common construction variables illustrated in Table 2. This study normalizes construction assemblies between parametric and baseline models to analyze building geometry, orientation, and building layout; furthermore, specific construction information for city-wide residential buildings is typically not recorded as frequently. Similarly, existing shading obstructions (buildings and trees) are not included in the parametric model comparison study in an effort to evaluate all parametric design types for 'worst case scenario' overheating. The intent for the parametric models is for a bottom-up UBEM to analyze vulnerability potential in multiple dwellings, not *specific* indoor heat stress values for every home in a city.

Table 3: Baseline building design summary

Building	Plan	FL	Floor Areas
1	H-shaped	1	FL.1: 184m^2 (1,980 feet^2)
2	L-shaped	2	FL.1: 281m^2 (3,025 feet^2); FL.2: 80.3m^2 (864 feet^2)
3	Rectangle	2	FL.1: 95.7m^2 (1,030 feet^2); FL.2: 86.4m^2 (930 feet^2)

In addition, the baseline and parametric model simulations do not include air-conditioning or natural ventilation from open windows in order to simulate the 'worst case scenario' condition where air-conditioning is not present and windows are unable to be opened; this is a particular concern during peak summer weather and heat wave events. With that in mind, the simulation period includes a three-day range (July 18-20) where the daily high dry-bulb temperature exceeds 32°C (90°F) and represents the hottest period in the weather data file; each simulation also includes a 7-day warm-up period just prior to the 3-day simulation period. The weather data used for baseline and parametric model simulations is the TMY3 data file from Cleveland Hopkins International Airport (US Department of Energy Building Technology Office, 2016). This study does not adjust the weather data for urban heat island effects.

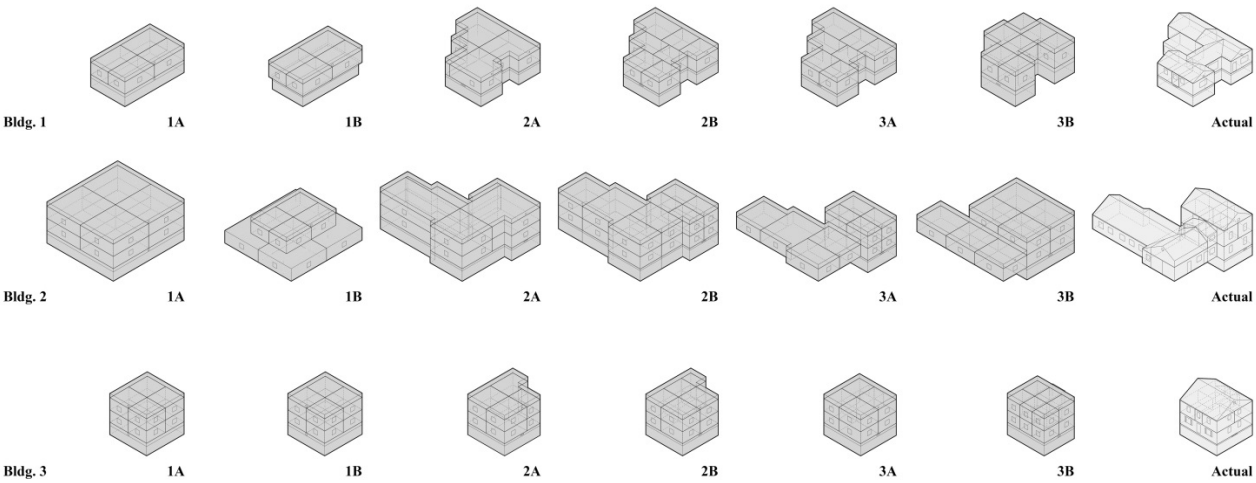

Figure 2: Example geometry for baseline Buildings (1, 2, and 3) and their six parametric energy model options

4) 'Flex' parametric model to represent baseline

Each parametric model type is 'flexed' to represent each of the three baseline houses using the corresponding GIS and/or existing building survey data; a total of 18 stock parametric energy models resulted from this process. The local county (Cuyahoga County) property database provided the building archetypal data (floor areas, CAD layouts, room types, etc) for each of the parametric models in relation to the baseline models (Cuyahoga County, 2016). Each model is simulated under the same weather and operating conditions as the baseline models. For this study, neighboring building geometries are included as shading objects; the greater UBEM overheating vulnerability study would utilize the neighboring parametric model for shading objects. Figure 2 illustrates how the parametric models flex in relation to baseline Building 2.

5) Calculate heat stress metric from model outputs

This study utilizes both internal WBGT and operative temperature (OT) as heat stress metrics. WBGT is a heat-stress metric used in occupational safety standards in conjunction with maximum temperature thresholds based on worker metabolic rates (International Organization for Standardization, 1989). OT is the overheating criteria for both the ASHRAE-55 and the BS EN 7730 adaptive comfort models (ASHRAE, 2013; BSI, 2007). This study analyzes hourly WBGT and OT values for a 3-day overheating period: July 18-20.

Operative temperature is a direct energy model output, however to obtain WBGT values from an energy models, a series of post-simulation calculations are required. An energy modeling study by Holmes (2016) validated a method to calculated indoor WBGT values using a WBGT equation validated by Lemke (2013) and the energy model outputs for dry-bulb temperature, relative humidity, and indoor air speed. Using the process outlined by Holmes, this paper calculates indoor WBGT values using a related WBGT equation also validated by Lemke (2013) and indicated in Equation 1.

$$WBGT = 0.67Tpwb + 0.33Ta - 0.048 \log_{10}v\,(Ta-Tpwb). \quad (1)$$

Where: Tpwb = Psychrometric wet-bulb temp.
v = air speed
Ta = dry-bulb temperature

This paper calculates Tpwb values for Equation 1 inputs using Ta and Relative Humidity (RH) model outputs using Equation 2 (Stull, 2011)

$$Tpwb = Ta\ atan[0.151977(RH\% + 8.313659)^{1/2}] + atan(Ta + RH\%) - atan(RH\% - 1.676331) + 0.00391838(RH\%)^{3/2} atan(0.023101RH\%) - 4.686035 \quad (2)$$

Where: Ta = dry-bulb temperature
RH = Relative Humidity

Additionally, as indoor air-speed is not a direct model output, this paper assumes 0.3m/s (60 fpm) indoor air speed to simulate either a low-speed room fan or minimal occupant movement.

6) Compare models for accuracy

The accuracy analysis compares each baseline model with the six parametric models to determine how closely the stock parametric models represent the custom baseline models. The analysis calculates a linear correlation (R^2) and the coefficient of variation of the root mean squared error (CV-RMSE) for WBGT and OT values. Using ASHRAE Guideline 14-2014 as a reference, the study examines the proportion of variation and uncertainty between the models; the acceptance limit variation is $R^2 \geq 0.8$ and uncertainty or error of CV-RMSE $\leq 20\%$ (ASHRAE, 2014). The study compares both a southwest upper floor zone (presumed hottest) and a northeast ground floor zone (presumed coolest) for each model. Additionally, the comparison includes graphs illustrating the hourly indoor WBGT for each building and its associated options.

Results and Analysis

Table 4 illustrates the calculated R^2 and CV-RMSE values used to compare the six parametric model types with each of the three baseline models (Buildings 1, 2, and 3); the Table includes R^2 and CV-RMSE values generated from outputted OT values and calculated WBGT values for both a Northeast (NE) and Southwest (SW) room. Finally, Table 4 also highlights the resulting cells for R^2 and CV-RMSE values in relation to the acceptance limits ($R^2 \geq 0.8$; CV-RMSE $\leq 20\%$) using a gradient white/grey (strong/weak) scale; additionally, cells where values exceeding the limits render as red. In other words, the lighter grey the cell is, the stronger the value, with red being out of bounds.

The graphs in Figure 3 illustrate the hourly indoor WBGT for each model of the case study buildings and their associated parametric modeling options; these graphs also include the calculated outdoor WBGT (in shade) for reference values. The graphs only illustrate the first day of the simulation period (July 18) because it contained the hottest exterior dry-bulb temperature during the simulation period.

The results indicate that, with a few exceptions, the study has acceptable proportion of variation and uncertainty of error for the 144 values generated (3 houses x 6 models x 2 rooms x 2 overheating metrics x 2 analysis measures). Only 11 of the 144 values (7.6%) exceeded specified limit and six of those values were from the same category (Building 1, Northeast room, OT, and R^2).

For the regression test in Building 1, the northeast room in all models does not produce acceptable results for R^2; this is likely because the northeast room in the existing building is a large open family room with eastern, southern and limited western exposure. The nighttime OT values for the baseline building model were cooler (~1.7°C/3°F at midnight) than the OT values in the northeast rooms for all the stock models; this is likely due to a larger zone exterior wall surface area having

greater infiltration rate and heat loss to the exterior.

Table 4: R2 and CV-RMSE values when comparing parametric and baseline models for OT and WBGT

Building 1 (1-storey, H-Shaped)

OT	1A	1B	2A	2B	3A	3B
R2 (NE)	0.6389	0.6610	0.4977	0.6158	0.6617	0.6389
CV-RMSE (NE)	7.09%	8.07%	7.86%	7.55%	5.31%	6.12%
R2 (SW)	0.8155	0.8402	0.7030	0.8916	0.8808	0.9792
CV-RMSE (SW)	4.55%	5.15%	5.26%	5.43%	4.48%	5.61%
WBGT	1A	1B	2A	2B	3A	3B
R2 (NE)	0.9145	0.9229	0.8770	0.9026	0.8800	0.9138
CV-RMSE (NE)	3.44%	3.81%	4.05%	3.81%	3.34%	2.87%
R2 (SW)	0.8992	0.9107	0.8588	0.9229	0.9179	0.9595
CV-RMSE (SW)	3.32%	3.15%	3.92%	2.84%	2.99%	2.37%

Building 2 (2-storey, L-Shaped)

OT	1A	1B	2A	2B	3A	3B
R2 (NE)	0.8358	0.9154	0.9680	0.9876	0.9885	0.9261
CV-RMSE (NE)	12.07%	32.83%	2.52%	3.02%	5.17%	10.69%
R2 (SW)	0.7470	0.9142	0.8398	0.8850	0.9750	0.8441
CV-RMSE (SW)	6.75%	7.44%	7.33%	6.21%	2.20%	6.23%
WBGT	1A	1B	2A	2B	3A	3B
R2 (NE)	0.7977	0.8577	0.9730	0.9874	0.9748	0.8585
CV-RMSE (NE)	6.32%	21.44%	1.72%	2.16%	2.34%	5.58%
R2 (SW)	0.8516	0.9041	0.9214	0.9353	0.9910	0.8985
CV-RMSE (SW)	4.91%	4.47%	5.30%	4.48%	1.24%	3.72%

Building 3 (2-storey, Rectangle shaped)

OT	1A	1B	2A	2B	3A	3B
R2 (NE)	0.9819	0.9778	0.9815	0.9060	0.9524	0.9481
CV-RMSE (NE)	3.38%	1.74%	10.40%	2.63%	4.08%	2.26%
R2 (SW)	0.9559	0.9636	0.9468	0.9556	0.9541	0.9350
CV-RMSE (SW)	6.45%	6.09%	8.01%	5.94%	6.00%	9.11%
WBGT	1A	1B	2A	2B	3A	3B
R2 (NE)	0.9453	0.9838	0.8864	0.9655	0.9562	0.9460
CV-RMSE (NE)	2.23%	1.84%	5.05%	2.04%	3.36%	3.63%
R2 (SW)	0.9272	0.9287	0.9339	0.9289	0.9276	0.9121
CV-RMSE (SW)	3.97%	3.92%	4.69%	3.81%	3.81%	5.36%

Similarly, the Building 1 Model 2A, southwest room fails the R2 test and has weak results in the CV-RMSE for both OT and WBGT. The 2A model subdivides the building footprint into four zones that originate from the footprint centroid; given that Building 1 is "H" shaped, the resulting southwest zone's plan is "L" shaped. Similar to the northeast zone, the 2A southwest zone has significant exterior wall and nighttime heat loss. However, all six models for Building 1 have acceptable WBGT values for both the northeast and southwest for both R2 and CV-RMSE.

Overall, the CV-RMSE results indicate that WBGT values are typically more accurate than OT for all three building types and model types. This is probably due to the use of both TA and RH in determining the final value as opposed to relying on one metric. The only two instances where WBGT values fall out of bounds is for Building 2, Northeast room, Models 1A and 1B. For this instance, illustrated in Figure 2, the baseline building is L shaped with a smaller second floor footprint; however, both models use square footprints for the first floor and either extrude that square to the second floor (1A) or offset the perimeter of the square for the second floor (1B). When examining the existing building, the Northeast first floor room is directly under a roof, whereas the 1A and 1B models assume the second floor sits either completely or partly over the northeast room. This difference in exposure to an attic space likely affected the heat flow significantly. The southwest room passed both R2 and CV-RMSE tests, but the Category 1 models are weaker than the other four models.

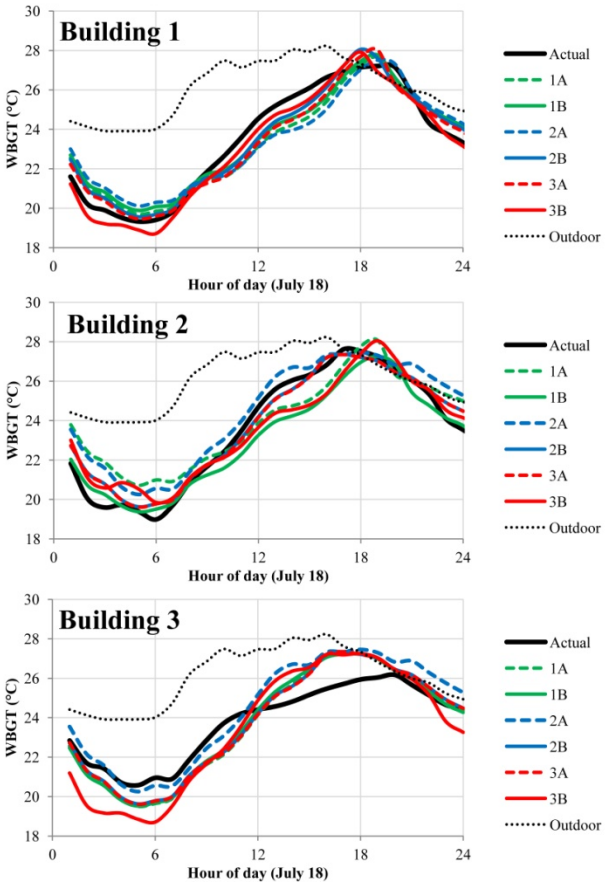

Figure 3: Hourly WBGT values for Buildings 1, 2, & 3 in the Southwest, top floor rooms.

Finally, Building 3 has the strongest CV-RMSE results for all six models types in that all evaluation categories contain acceptable results for the whole simulation period and during peak temperatures (Table 5); however Building 1 also exhibits strong peak CV-RMSE values. Unlike the other two baseline buildings, Building 3 is primarily rectilinear in plan, has a second floor that has essentially the same footprint as the first floor, and contains a simple 4-square zone layout. The only exception to the consistent footprint is a small 1-story kitchen addition off the east side of the building. Furthermore, the northeast room in Building 3 falls within the primary rectangular shape of the building, has an occupied floor above, and is a simple corner zone with one exterior wall; the northeast rooms in Building 1 and 2 both have attics overhead and the Building 1 zone is a wide-open room covering half the floor plan. The uniform arrangement of the Northeast zone in Building 3 allows Models 1A and 1B to replicate the existing building quite closely. Table 4 indicates that Model 2A is within acceptable limits, but is notably the least accurate in replicating the baseline model; this is likely

due to the footprint including the kitchen addition, which is extruded onto both floors and similarly absorbed into the simple 4-zone layout of the stock model. Similarly, Model 3B overemphasizes the kitchen addition and minimizes the northeast and southwest zone scales due to the 3x3 zone layout.

The peak temperature CV-RMSE analysis indicates that calculated OT and WBGT temperatures from parametric model types 2A, 2B, 3A, and 3B are within an acceptable range of baseline model temperatures. Similar to the full simulation periods analysis, Model 1B indicates the most variability across the three building case studies (including unacceptable results for the Building 2 case study.

Table 5: CV-RMSE values when comparing parametric and baseline models for Peak OT and WBGT

Building 1 (1-storey, H-Shaped) - PEAK TEMPERATURE

OT	1A	1B	2A	2B	3A	3B
CV-RMSE (NE)	0.92%	1.04%	2.71%	1.55%	8.16%	3.08%
CV-RMSE (SW)	2.54%	3.90%	0.25%	7.40%	5.20%	10.39%
WBGT	1A	1B	2A	2B	3A	3B
CV-RMSE (NE)	4.35%	5.21%	4.36%	4.75%	0.39%	2.52%
CV-RMSE (SW)	1.87%	0.67%	3.06%	1.56%	0.49%	2.72%

Building 2 (2-storey, L-Shaped) - PEAK TEMPERATURES

OT	1A	1B	2A	2B	3A	3B
CV-RMSE (NE)	15.92%	37.51%	2.10%	4.10%	5.96%	14.08%
CV-RMSE (SW)	7.93%	11.07%	0.04%	1.00%	2.42%	10.43%
WBGT	1A	1B	2A	2B	3A	3B
CV-RMSE (NE)	7.81%	27.63%	0.62%	1.63%	3.00%	7.57%
CV-RMSE (SW)	5.91%	9.53%	0.85%	0.84%	2.13%	6.74%

Building 3 (2-storey, Rectangle shaped) - PEAK TEMPERATURE

OT	1A	1B	2A	2B	3A	3B
CV-RMSE (NE)	4.77%	1.41%	12.83%	1.96%	2.75%	1.56%
CV-RMSE (SW)	8.37%	7.63%	15.47%	7.99%	7.83%	11.57%
WBGT	1A	1B	2A	2B	3A	3B
CV-RMSE (NE)	0.66%	3.84%	0.93%	1.24%	4.84%	6.39%
CV-RMSE (SW)	4.45%	4.07%	7.81%	4.47%	4.42%	4.50%

An analysis of the hourly WBGT values, illustrated in Figure 3, indicates that the indoor WBGT values for the Building 1 and 2 parametric models more closely track their corresponding baseline building models when compared to the parametric models associated with Building 3. The parametric models for Buildings 1 and 2 exhibit a similar pattern of hourly results that include relative close tracking during nighttime and daytime hours, as well as a slightly higher and more delayed peak WBGT values in the later afternoon. The hourly WBGT generated by the parametric models for Building 3 indicate cooler nighttime and warmer mid-afternoon values compared to the baseline model. Of the three models, Building 1 exhibited the closest hourly value tracking between parametric and baseline models. When examining the different parametric design options in regards to hourly WBGT values, the three design options that utilize specific building footprint dimensions (Models 2A, 2B, and 3A) appear to track the baseline building the closest across all the building examples.

Discussion

All six stock parametric energy models for single-family houses produce acceptable indoor OT and WBGT values for use in overheating analysis provided the parametric models use the appropriate property information inputs. As Table 3 illustrates, the six modeling methods use different combinations of input parameters in an effort to represent a variety of property database information available to the modeler. The study's intention is not to isolate one modeling methodology as the ultimate solution for use in UBEM overheating studies; rather it identifies the viability of different modeling methods based on an assumption that different cities have different property data that would be available for parametrically modeling the local housing stock. Even though this study normalizes building construction assembly and occupant load variables, the analysis addresses a variety of building geometry options to provide alternative to modelers for UBEM studies.

With that said, even though all six models presented are strong in certain instances (i.e., rectangular, 2-story buildings), models 2B, 3A, and 3B tend to be stronger overall with all three of the baseline house types analyzed (1- story, split-level, 2-story) as shown in Table 4; much of the error occurs due to building geometry arrangements. Similarly, Models 2B and 3A, which utilize actual footprint dimensions, more accurately generate hourly WBGT values as indicated in the analysis based on Figure 3 data. Though the models 1A and 1B (4-zone, square) create acceptable results for 1 and 2-story buildings, they are not as successful at representing the split-level home category; model 1B has particularly high uncertainty error likely due to the smaller split-level second floor being centered over the lower floor. Similarly, models 1A, 1B, and 2A have weak R^2 results in non-rectilinear buildings due to their simple 4-zone subdivision; however, uncertainty error does remain acceptable for all three models. Given this evaluation, model 1B appears to be generally unacceptable due to high error in representing a split-level home. Assuming that identifying split-level homes (with or without GIS or CAD layouts) is difficult for a parametric UBEM study, the authors recommend not using Model 1B for UBEM studies for indoor overheating assessment.

Furthermore, all models generated weak R^2 values for OT in the northeast room of Building 1. This result reflects a weakness in all the modeling methods to address larger rooms that contain more than two external wall surfaces. However, the authors believe the modeling methods are still valid for the following reasons: 1) the OT error and WBGT results are still above a R^2 of 0.8; 2) most of the remaining results for other rooms and buildings also have acceptable results, and 3) an assumption that occupants would shelter-in-place during a heat wave in rooms with less external exposure. One avenue of future research is the development of stock parametric models that divide zones based on internal room layouts, in the event that a

city has appropriate data documenting internal room arrangements and sizes.

While the methods presented successfully demonstrate stock parametric models representing the behavior of detailed models, even detailed models struggle to produce specific results for identifying heat-vulnerable dwellings due to numerous variables (occupant behavior, microclimate, building idiosyncrasies, etc). Additionally, this study does not specifically address building construction assemblies, external vegetated shading, and natural ventilation among other related variables. These concerns represent opportunities for further investigation and expansion of the stock model parameters.

The primary takeaway of this study is a proof of concept for using parametric multi-zone energy models in UBEM housing overheating analyses; using stock models in a UBEM overheating analyses does not inherently require highly detailed model results. With this information, urban planners, public health officials, and emergency managers conducting UBEM overheating studies could identify which buildings were most at risk, not the exact conditions within a house.

Though including more parameters and variables will inherently make the stock models more robust, the basic stock parametric energy models presented offer the opportunity for urban planners and city officials to investigate overheating potential across the housing stock. Feasibly, a UBEM could automatically construct every single-family residential building in a city's property database using one or more of the parametric energy models and simulate an ensuing heat event using historical or projected weather data. This type of UBEM study would include city-level data, such as shading obstructions from neighboring buildings and trees, ground surface materials, and urban form and orientation to further refine the microclimatic variables that affect each residential model. Resulting room data for each home could then be assessed using predetermined overheating criteria (i.e., three or more rooms > 28°C / 82.5°F WBGT), and resulting vulnerability assessment could then be fed into a GIS database to map which homes are most at risk. Emergency management officials could then use this relative risk map to help prioritize which households to contact during a heat wave. However, this paper does not address linking the stock models to GIS databases; further programming development is required to automate stock model creation and risk mapping through GIS systems.

A few additional limitations to this study exist and offer opportunities for improvement. As previously stated, understating or assuming building operations and controls presents a significant hurdle; further study could develop operation assumptions based on occupant demographics, building age and construction type, and more specific microclimate data. Similarly, the models should consider archetypal construction assemblies and building finishes as input parameters; including construction assembly inputs would provide modelers with an opportunity to link a city's construction quality indicators with predefined construction archetypal data for use in each model. Additionally, this study did not use shading obstructions in an effort to maximize internal heat gain for simulation of indoor overheating conditions for purposes of this model design comparison; however, shading is an extremely important factor and should not be included in all UBEM studies attempting to ascertain potential overheating vulnerability. Finally, the models assume 1 or 2 windows per zone; further development of building surveys could provide an opportunity to more accurately represent window to wall ratio for each building.

Additional opportunities exist to expand the study to include greater precision and application. First, CityGML databases offer an opportunity to collect 3d information about building envelopes; additional stock models could incorporate this data and not rely solely on GIS footprints (Open Geospatial Consortium, 2012). Additionally, a UBEM overheating analysis could address the heat island effect and shading from vegetation by linking the energy models with GIS land cover data and LIDAR databases respectively. Furthermore, this study could expand stock model development into other residential buildings such as town homes, duplexes, multi-family (low, mid, high-rise), and office buildings. Finally, further work is needed to optimize an overheating metric for use in residential buildings; the WBGT and Predicted Heat Strain metrics are typically used in workplace conditions but have yet to be applied in residential applications (Holmes S. H., 2016).

Conclusion

This study evaluates the ability of six unique parametric multi-zone energy models to mimic the behavior of detailed single-family home energy models for use in citywide overheating vulnerability studies. When evaluated for operative temperature and wet-bulb globe temperature overheating metrics, five of the six models prove to be viable options when compared to custom energy models of three existing homes in Cleveland Ohio, USA; models that include building footprint and differentiate floor areas prove more reliable. Though precise prediction of indoor overheating conditions is not realistic, these models offer a first pass for urban energy modelers, urban planners, or emergency managers to evaluate which residences are at most risk during a prolonged heat event.

Acknowledgements

Support for portions of this research was provided by the National Science Foundation (NSF) Graduate Research Fellowship under Grant Number DGE 0718128. Support was also received from both the Graham Sustainability Institute, the Energy Institute at the University of Michigan, and the University of Hartford.

The Kresge Foundation provided funding for climate resilience planning from their Climate Resilience and

Urban Opportunity Initiative to Cleveland Neighborhood Progress, the City of Cleveland, Kent State University, and the University at Buffalo.

The authors would like to thank the the three reviewers for their valuable feedback and suggested edits to improve this article. We would also like to thank the anonymous homeowners in Cleveland, Ohio for allowing us access to their houses to take thermal environmental data.

Nomenclature

CAD: Computer Aided Design
CV-RMSE: Coefficient of Variation Root Mean Squared Error
FL: Floor level
GIS: Geographic Information Systems
NE: Northeast
OT: Operative Temperature
R^2 or R2: Regression
RH: Relative Humidity
SW: Southwest
TA: Dry-bulb temperature
TMY3: Typical Meteorological Year 3
UBEM: Urban Building Energy Model
WBGT: Wet-bulb globe Temperature

References

ASHRAE. (2013). *ANSI/ASHRAE Standard 55:2013 - Thermal Environmental Conditions for Human occupancy.* Atlanta, GA: American Society of Heating, Ventilation, Refrigeration, and Air-conditioning Engineers.

ASHRAE. (2014). *Guideline 14-2014, Measurement Of Energy, Demand, And Water Savings.* Atlanta, GA: American Society of Heating, Refrigerating & Air Conditioning Engineers.

BSI. (2007). *BS EN 15251:2007 Indoor environmental input parameters for design and assessment of energy performance of buildings addressing indoor air quality, thermal environment, lighting and acoustics.* London: British Standards Institution.

Building Resiliency Task Force. (2013). *Report to Mayor Michael R. Bloomberg & Speaker Christine Quinn.* New York City: Urban Green.

Cerezo, C., Sokol, J., Reinhart, C., & Al-Mumin, A. (2015). Three methods for charatcterizing buildoing archetypes in urban energy simulation. A casey study in Kuwait City. *Building Simulation 2015* (pp. 2873-2880). Hyperbad, India: International Building Performance Simulation Association.

Chuang, W.-C., & Gober, P. (2015). Predicting Hospitalization for Heat-Related Illness at the Census-Tract Level: Accuracy of a Generic Heat Vulnerability Index in Phoenix, Arizona (USA). *Environ Health Perspect , 123* (6), 606-612.

Cuyahoga County. (2016). *Real Property Information.* Retrieved November 16, 2016, from Cuyahoga County Fiscal Officer: https://fiscalofficer.cuyahogacounty.us/en-US/REPI.aspx

Dogan, T. (2016). *ARCHSIM*. Retrieved January 6, 2016, from http://archsim.com

Ellis, P. (2016). A Parametric Tool for Community-Scale Modeling. *ASHRAE and IBPSA-USA SimBuild 2016.* Salt Lake City, UT: ASHRAE and IBPSA-USA.

Holmes, S. H. (2016). Energy model validation for indoor occupant heat stress analysis. *ASHRAE and IBPSA-USA SimBuild 2016.* Salt Lake City, UT: ASHRAE and IBPSA-USA.

Inteligent Energy Europe. (2012). Typology Approach for Building Stock Energy Assessment. Darmstadt, Germany.

Intergovernmental Panel on Climate Change. (2014). *Climate Change 2014:Impacts, Adaptation, and Vulnerability IPCC Working Group II Contribution to AR5.* New York: United Nations, Intergovernmental Panel on Climate Change.

International Organization for Standardization. (1989). *ISO 7243:1989: Hot environments - Estimation of the heat stress on working man, based on the WBGT-index (wet bulb globe temperature).* Geneva, SUI: International Organization for Standardization.

Lemke, B., & Kjellstrom, T. (2013). Calculating Workplace WBGT from Meteorological Data: A Tool for Climate Change Assessment. *Industrial Health , 50*, 267-278.

Loughnan, M. E., Tapper, N. J., Phan, T., Lynch, T., & McInnes, J. A. (2013). *A spatial vulnerability analysis of urban populations during extreme heat events in Australian capital cities.* Gold Coast: National Climate Change Adaptation Research Facility.

ONeill, M., & Ebi, K. (2009). Temperature extremes and health: impacts of climate variability and change in the United States. *Journal of Occupational & Environmental Medicine , 51* (1), 13-25.

Open Geospatial Consortium. (2012). *City Geography Markup Language (CityGML) Encoding Standard.* Wayland, MA, USA: Open Geospatial Consortium.

Parker, A., Benne, K., Brackney, L., Hale, E., Macumber, D., Schott, M., et al. (2014). A Parametric Analysis Tool for Building Energy Design Workflows: Application to a Utility Design Assistance Incentive Program. *The Next Generation: Reaching for High Energy Savings* (pp. 263-274). Pacific Grove, CA: ACEEE.

Reid, C. E., O'Neill, M. S., Grondlund, C. J., Brines, S. J., Brown, D. G., Diez-Roux, A. V., et al. (2009).

Mapping community determinants of heat vulnerability. *Environ Health Perspecitve , 117* (11), 1730-1736.

Reinhart, C., & Cerezo, C. (2016). Urban building energy modeling – A review of a nascent field. *Building and Environment* , 196-202.

Robert McNeel & Associates. (2016). *Rhinoceros*. Retrieved Janurary 6, 2016, from https://www.rhino3d.com/

Rosenthal, J. K., Kinney, P. L., & Metzger, K. B. (2014). Intra-urban vulnerability to heat-related mortality in New York City,1997–2006. *Health & Place , 30*, 45-60.

Seroka, C., Kaiser, P., & Heany, J. (2011). *Mapping Heat Vulnerability in Michigan*. Okemos, MI: Michigan Public Health Institute.

Stull, R. (2011). Wet-Bulb Temperature from Relative Humidity and Air Temperature. *Journal of Applied Meteorology and Climatology* (50), 2267-2269.

Tian, W., Rysanek, A., Choudhary, R., & Heo, Y. (2015). High resolution energy simulations at city scale. *Building Simulation 2015* (pp. 239-246). Hyperbad, India: International Building Performance Simulation Association.

US Department of Energy Building Technology Office. (2016). *Energy Plus*. (US Department of Energy, Building Technologies Office) Retrieved January 6, 2016, from https://energyplus.net/

White Box Technologies. (2016). *Historical Weather Files.* Retrieved from White Box Technologies: Historical weather data for energy calculations: http://weather.whiteboxtechnologies.com/